JOURNAL OF Materials CHEMISTRY

Synthesis, crystal structure, and magnetic properties of $NH_4CuPO_4{\cdot}H_2O$

Ainhoa Pujana,[a] Jose Luis Pizarro,[a] Luis Lezama,[b] Aintzane Goñi,[b] María Isabel Arriortua*[,a] and Teófilo Rojo[b]

[a]*Dpto. Mineralogía y Petrología, Universidad del País Vasco, Bilbao 48080, Spain*
[b]*Dpto. Química Inorgánica, Universidad del País Vasco, Bilbao 48080, Spain*

In this paper is described the synthesis and characterization of a new layered phosphate, $NH_4CuPO_4{\cdot}H_2O$, and its magnetic properties. Its crystal structure has been solved at room temperature. It crystallizes in the $P2_1/a$ monoclinic space group, with $a=7.3907(8)$, $b=7.5191(6)$, $c=8.651(1)$ Å, $\beta=94.54(1)^\circ$ and $Z=4$. The compound presents a layered structure, with copper phosphate sheets linked by NH_4^+ cations. These layers are parallel to the (001) plane and are interconnected by hydrogen bonds with the NH_4^+ cations. The layers are formed by centrosymmetric dimers of CuO_5 edge-sharing distorted square pyramids, crosslinked by corner-sharing phosphate tetrahedra. Each copper(II) cation is bonded to three phosphate oxygens and one water molecule forming the base of the square pyramid, and a symmetry related phosphate oxygen in the axial position. The crystal structure of $NH_4CuPO_4{\cdot}H_2O$ is related to the layered dittmarite ($NH_4MgPO_4{\cdot}H_2O$) type structure. However, in the dittmarite family there are MO_6 octahedra separated by the phosphate groups. The title compound is the first one related to the dittmarite family which exhibits layers formed by centrosymmetric Cu_2O_8 dimers crosslinked by phosphate tetrahedra. The IR data of this layered phosphate are in good agreement with the symmetry observed in the phase. EPR data and magnetic studies show the existence of antiferromagnetic interactions and the presence of predominant short range interactions. In spite of the layered structure exhibited by the compound, the magnetic study indicates that the magnetic behaviour is consistent with a dimeric structure with a J/k value of 4.93 K. A 2D ordering, as exhibited by other related compounds, may be reached at temperatures lower than 1.8 K.

Introduction

Transition metal phosphates offer a considerable number of different structures which can give rise to practical applications such as ionic exchange, ionic conductivity, *etc*., and interesting magnetic properties.[1] Only a limited number of phosphates form two-dimensional (2D) layered structures. Both the low dimensionality and the intercalation properties of some of these layered phosphates make them attractive and exciting for materials scientists. An example of this interest is the extensive study of the intercalation behaviour of the layered vanadyl phosphates[2,3] or α-zirconium phosphates.[4–6]

The well known series of compounds $M^IM^{II}PO_4{\cdot}H_2O$ ($M^I=NH_4$, K; $M^{II}=$Mn, Fe, Co, Ni)[7] related to the dittmarite $NH_4MgPO_4{\cdot}H_2O$ mineral, has been of interest because of the strongly defined layered crystal structures of these phases. All these compounds crystallize in the rhombic space group $Pmn2_1$. The structure consists of approximately square-planar sheets of M^{II} ions, coordinated in a severely distorted octahedron by five phosphate oxygens and one water molecule, separated by the M^I cation. This arrangement should afford interesting 2D magnetic interactions. In general, the magnetic susceptibility and specific heat results obtained for these phases show an essentially 2D antiferromagnetic exchange coupling, which becomes of a more 3D behaviour with decreasing temperature.[8,9] However, a study of the magnetic behaviour of the manganese compound[10] showed a crossover in the power law dependence of the magnetization with temperature. This result was attributed to a crossover in the lattice dimensionality from 2D to 3D at low temperatures. On the other hand, magnetic and Mössbauer studies of the $NH_4FePO_4{\cdot}H_2O$ compound[11,12] showed, at low temperatures, two different regimes. One of them involves a short-range ordered region at $70>T/K>26$ and the second is a long-range ordered region below 26 K, with an uniaxial antiferromagnetic state with the axis nearly parallel to the layer stacking direction. These results may be explained by the existence of superexchange pathways between the magnetic layers through the intercalated NH_4^+ ions.

In this paper, we report the crystal structure and magnetic properties of a new layered phosphate, $NH_4CuPO_4{\cdot}H_2O$. The crystal structure of this compound shows sheets formed by dimers of CuO_5 edge-sharing square pyramids, crosslinked by the phosphate tetrahedra. This fact is different from that observed for the dittmarite family in which the $[MO_6]$ octahedra are separated by the phosphate groups.[7] As far as we are aware, the title compound is the first one related to the dittmarite family which exhibits layers formed by centrosymmetric $[Cu_2O_8]$ dimers crosslinked by phosphate tetrahedra, giving rise to unusual magnetic properties with respect to those observed in this kind of compound.

Experimental

Preparation of the $NH_4CuPO_4{\cdot}H_2O$ compound

$NH_4CuPO_4{\cdot}H_2O$ was synthesized using a method derived from that given by Basset and Bedwell.[13] An aqueous solution of $CuCl_2{\cdot}2H_2O$ (0.01 M) was added to a large excess of a saturated $(NH_4)_2HPO_4$ solution (0.15 M). The resulting precipitate was digested. It was separated by filtration, and washed with water and diethyl ether. Blue prismatic crystals suitable for X-ray analysis were obtained. The elemental analysis was carried out with a Perkin-Elmer 2400 CHN analyzer: found H 3.2%; N 7.8%; calc: H 3.4%; N 8%. The copper elemental analysis was performed by absorption spectroscopy on Cu^{II} (Perkin-Elmer 3030B spectrophotometer) Found: Cu 35%; calc: Cu 36%.

Structure determination and refinement of $NH_4CuPO_4{\cdot}H_2O$

A single crystal of the $NH_4CuPO_4{\cdot}H_2O$ compound ($0.14\times0.18\times0.02$ mm) was mounted on an Enraf-Nonius CAD-4 automatic diffractometer using Mo-Kα radiation mon-

ochromated by graphite ($\lambda = 0.71069$ Å). The measurements were performed at room temperature (295 K). Crystal data and structural details are summarized in Table 1. The unit-cell parameters were least-squares refined using 25 reflections in the range 7°–13° θ. Four standard reflections were monitored periodically for crystal deterioration and/or misalignment. 2880 reflections were measured with $1° < \theta < 30°$, yielding 1397 independent reflections ($R_{int} = 0.070$). Empirical absorption corrections were applied to the data.[14]

The crystal structure was solved by the Patterson method using scattering factors and anomalous dispersions taken from ref. 15. The positions of copper and phosphorus atoms were found using sharpened Patterson functions (SHELX-86).[16] Successive Fourier synthesis (SHELX-93)[17] allowed us to locate all other non-hydrogen atoms. The calculations were performed, initially, with isotropic, and then with anisotropic thermal parameters. Hydrogen atoms were located by difference Fourier synthesis. Refinement was carried out using F^2. Final refinement led to convergence at $R = 0.021$ and $wR_2 = 0.047$.

The final fractional atomic coordinates and displacement parameters of the title compound are given in Table 2. Selected interatomic distances are shown in Table 3. The geometric calculations were performed with the programs PARST[18] and BONDLA[19] and molecular illustrations were drawn with the ATOMS[20] program. Full crystallographic details, excluding structure factors have been deposited at the Cambridge Crystallographic Data Centre (CCDC). See Information for Authors, Issue 1. Any request to the CCDC for this material should quote the full literature citation and the reference number 1145/80.

Table 1 Crystallographic data for the $NH_4CuPO_4 \cdot H_2O$ compound

formula	$NH_4CuPO_4 \cdot H_2O$
M_r	194.57
crystal system	monoclinic
space group (no.)	$P2_1/a$ (14)
a/Å	7.3907(8)
b/Å	7.5191(6)
c/Å	8.651(1)
β/°	94.54(1)
V/Å^3	479.23
Z	4
$F(000)$	388
$\rho_{calc.}$/g cm^{-3}	2.697
T/K	295
μ/cm^{-1}	48.20
diffractometer	Enraf-Nonius CAD4
radiation (λ/Å)	Mo-Kα (0.71069)
scan type	$\omega/2\theta$
h, k, l range collected	10, ±10, ±12
2θ range/°	2–60
reflections collected	2880
R_{int}	0.070
unique reflections	1397
reflections with $I \geqslant 2.5\sigma(I)$	1397
no. of parameters	93
R	0.021
wR_2	0.047

Table 2 Fractional atomic coordinates and equivalent displacement parameters (Å^2) for the $NH_4CuPO_4 \cdot H_2O$ compound

atom	x	y	z	$B_{eq}{}^a$/Å^2
Cu	0.06688(4)	0.19161(4)	0.03714(3)	0.76(1)
P	0.17416(8)	0.54653(7)	0.18885(6)	0.54(1)
N	0.02779(32)	0.77052(31)	0.52824(26)	1.33(5)
O(1w)	0.19080(24)	0.06444(23)	0.22396(20)	1.09(3)
O(2)	0.03234(22)	0.39467(20)	0.16567(9)	0.89(3)
O(3)	0.24163(24)	0.55062(22)	0.35987(18)	1.07(3)
O(4)	0.17017(21)	0.00658(21)	−0.08650(19)	0.94(3)
O(5)	−0.08229(24)	0.27561(20)	−0.14512(19)	1.13(4)
H(1)	0.151(5)	−0.028(4)	0.02033(42)	2.8(7)
H(2)	0.314(5)	0.057(5)	0.2151(39)	2.8(7)
H(3)	0.97(5)	0.695(4)	0.4794(39)	2.5(5)
H(4)	−0.066(5)	0.818(4)	0.4630(36)	2.5(5)
H(5)	−0.011(5)	0.726(5)	0.5911(42)	2.5(5)
H(6)	0.098(5)	0.862(5)	0.5597(39)	2.5(5)

$^a B_{eq}{}^a/\text{Å}^2 = (8\pi^2/3)[U_{22} + 1/\sin^2\beta(U_{11} + U_{33} + 2U_{13}\cos\beta)]$.

Physical measurements

IR spectra (KBr pellets) were obtained with a Nicolet FT-IR 740 spectrophotometer in the 400–4000 cm^{-1} region. Thermal analyses were carried out with a Perkin-Elmer 7 System. Crucibles containing 20 mg were heated at 5 °C min^{-1} under a nitrogen atmosphere. A Bruker ESP300 spectrometer operating at X and Q bands and equipped with standard Oxford low temperature devices was used to record the EPR powder spectra of the compound at different temperatures. The magnetic field was calibrated by a NMR probe and the frequency inside the cavities was determined with a Hewlett-Packard 5352B microwave frequency counter. Magnetic susceptibility measurements were performed on powdered samples between 1.8 and 300 K with a Quantum Design MPMS-7 SQUID magnetometer. The magnetic field used in the experiments was 0.1 T, a value at which the magnetization *versus* magnetic field curve was still linear at 1.8 K. Experimental susceptibility values were corrected for the diamagnetic contributions and for the temperature-independent paramagnetism.

Results and Discussion

Crystal structure of $NH_4CuPO_4 \cdot H_2O$

$NH_4CuPO_4 \cdot H_2O$ presents a layered structure with copper phosphate sheets separated by NH_4^+ cations, as shown in Fig. 1. The layers are formed by $[Cu_2O_8]$ centrosymmetric dimers of CuO_5 edge-sharing square pyramids, crosslinked by corner-sharing phosphate tetrahedra.

The copper(II) cations exhibit a distorted five coordinate square-pyramidal geometry, with the three phosphate oxygens [Cu—O(2),O(4),O(5): 1.918(1), 1.947(2), 1.956(2) Å] and the water molecule [Cu–O(1w): 2.032(2) Å] forming the base of the square pyramid, and a symmetry related phosphate oxygen of the second bridging group [Cu—O(4)^i: 2.364(2) Å (i = $-x$, $-y$, $-z$)] located in the axial position. The O—Cu—O angles are in the ranges 81.58°–105.22° (mean value of 90.8°) and 164.43°–169.35°. The base of the square pyramid is distorted, with deviations out of plane of −0.236(2) Å, −0.207(2) Å for O(1w) and O(5) respectively, and 0.182(2) Å, 0.187(2) Å for O(2) and O(4) respectively. The copper ion is in the basal plane, with a deviation of −0.0561(3) Å.

The Cu_2O_8 centrosymmetric dimers are formed by two square pyramids which share the O(4)—O(4)^i (i = $-x$, $-y$, $-z$) edge (Fig. 2). The existence of an inversion centre causes the Cu—O(4)—Cu^i—O(4)^i bridging unit to form a plane. In the dimeric unit, the copper(II) cations are separated from each other by 3.0972(5) Å. The bridging angle slightly deviates from orthogonality, with Cu—O(4)—Cu^i (i = $-x$, $-y$, $-z$) of 91.48°.

The PO_4 groups can be described as distorted tetrahedra. The P—O distances, with a mean value of 1.54 Å, range from 1.524(2) Å to 1.552(2) Å, and the O—P—O angles are in the range from 107.82(9)° to 111.44(9)° [mean value 109(2)°]. The PO_4 groups are connected to the copper square pyramid by the three oxygen vertices, O(2), O(4) and O(5). The fourth oxygen corner, O(3), is directed towards the interlayer space.

The NH_4^+ tetrahedra are quite regular, with mean N—H distances of 0.88(2) Å and mean H—N—H angles of 109(3)°. The NH_4^+ ions placed between the layers establish hydrogen bonds with three symmetrical O(3) atoms and one O(2) atom of the four adjacent phosphate groups of two facing layers. The N—O distances range from 2.778(3) to 2.990(3) Å.

Table 3 Selected bond lengths (Å) and angles (degrees) for the $NH_4CuPO_4 \cdot H_2O$ compound

	bond lengths		angles	
Cu coordination square pyramid	Cu—O(1w)	2.032(2)	$O(4)^i$—Cu—O(5)	88.32(6)
	Cu—O(2)	1.918(1)	$O(4)^i$—Cu—O(4)	88.69(6)
	Cu—O(4)	1.947(2)	$O(4)^i$—Cu—O(2)	105.22(6)
	Cu—O(5)	1.956(2)	$O(4)^i$—Cu—O(1w)	81.58(6)
	$Cu—O(4)^i$	2.364(2)	O(1w)—Cu—O(2)	89.16(7)
			O(1w)—Cu—O(4)	85.93(7)
			O(4)—Cu—O(5)	90.48(7)
			O(5)—Cu—O(2)	96.77(7)
			O(4)—Cu—O(2)	164.43(7)
			O(1w)—Cu—O(5)	169.35(7)
Cu dimer:	$Cu—Cu^i$	3.0972(5)	Cu—O(4)—Cu^i	91.48(1)
	$Cu—Cu^{iv}$	3.7982(6)	mean O—Cu—O (*ca.* 90)	90.8(1)
			mean O—Cu—O (*ca.* 180)	165(1)
phosphate tetrahedra	P—O(2)	1.552(2)	$O(3)—P—O(5)^{ii}$	109.05(9)
	P—O(3)	1.524(2)	$O(3)—P—O(4)^{iii}$	111.17(9)
	$P—O(4)^{iii}$	1.536(2)	$O(5)^{ii}—P—O(4)^{iii}$	111.44(9)
	$P—O(5)^{ii}$	1.536(2)	O(3)—P—O(2)	107.82(9)
			$O(5)^{ii}$—P—O(2)	109.17(9)
			$O(4)^{iii}$—P—O(2)	108.10(9)
ammonium tetrahedra	N—H	0.88(2)	H—N—H	109(3)

	donor—H	donor···acceptor	H···acceptor	donor—H···acceptor
hydrogen bonds				
interlayer bonds:	N—H(3)	N···O(3)	H(3)···O(3)	N—H(3)···O(3)
	0.895(35)	2.778(3)	1.886(35)	174(3)
	N—H(4)	$N···O(3)^v$	$H(4)···O(3)^v$	$N—H(4)···O(3)^v$
	0.93(3)	2.813(3)	1.895(33)	169(3)
	N—H(5)	$N···O(2)^{vi}$	$H(5)···O(2)^{vi}$	$N—H(5)···O(2)^{vi}$
	0.719(38)	2.990(3)	2.308(37)	159(4)
	N—H(6)	$N···O(3)^{vii}$	$H(6)···O(3)^{vii}$	$N—H(6)···O(3)^{vii}$
	0.891(36)	2.831(3)	1.942(35)	176(3)
interdimer bond:	O(1w)—H(2)	$O(1w)···O(2)^{iv}$	$H(2)···O(2)^{iv}$	$O(1w)—H(2)···O(2)^{iv}$
	0.918(40)	2.631(2)	1.744(40)	162(4)
intradimer bond:	O(1w)—H(1)	$O(1w)···O(5)^i$	$H(1)···O(5)^i$	$O(1w)—H(1)···O(5)^i$
	0.769(34)	2.749(2)	1.744(40)	171(9)

i = $(-x, -y, -z)$
ii = $(-x, 1-y, -z)$
iii = $(1/2-x, 1/2+y, -z)$
iv = $(1/2+x, 1/2-y, z)$
v = $(x-1/2, 3/2-y, z)$
vi = $(-x, 1-y, 1-z)$
vii = $(1/2-x, 1/2+y, 1-z)$

The water molecule forms intra- and inter-dimeric hydrogen bonds. The H(1) hydrogen establishes an intradimeric hydrogen bond with the $O(5)^i$ atom of the base of the symmetrical related square pyramid [$O(1w)···O(5)^i = 2.749(2)$ Å, $H(1)···O(5)^i = 1.744(40)$ Å, $O(1w)—H(1)···O(5)^i = 171(9)°$] and the H(2) hydrogen forms an interdimeric hydrogen bond with the $O(2)^{iv}$ atom of the symmetrical related dimer [$O(1w)···O(2)^{iv} = 2.631(2)$ Å, $H(2)···O(2)^{iv} = 1.744(40)$ Å, $O(1w)—H(2)···O(2)^{iv} = 162(4)°$] (i = $-x$, $-y$, $-z$), (iv = $1/2+x$, $1/2-y$, z) (Table 3).

The $NH_4CuPO_4 \cdot H_2O$ compound is related to the dittmarite family. The structure of this family is formed from sheets of distorted $M^{II}O_6$ (M^{II} = Mg, Mn, Fe, Co, Ni) corner-sharing octahedra bridged through three oxygen atoms of the phosphate tetrahedra. In the $NH_4CuPO_4 \cdot H_2O$ compound, the layers are formed by dimers of CuO_5 edge-sharing square pyramids, crosslinked by three phosphate tetrahedral groups (Fig. 3). In both cases, the fourth oxygen of the phosphate tetrahedra is not linked to the M^{II} cation and is directed towards the interlayer space. The five coordination to the copper(II) ion causes a distortion in comparison to the dittmarite structure. As a result, the intralayer unit cell parameters ($a = 7.3907$, $b = 7.5191$ Å) of the $NH_4CuPO_4 \cdot H_2O$ compound are almost equivalent to the intralayer unit cell diagonals of dittmarite ($a = 5.55$, $c = 4.80$ Å, diagonal = 7.33 Å) (see Fig. 3). The interlayer distances are similar for both compounds, however interlayer displacements with values of 8.85 Å and 8.609 Å are observed for dittmarite and $NH_4CuPO_4 \cdot H_2O$ respectively. This fact gives rise to a change in the crystalline system from rhombic to monoclinic.

Finally, note that the structure of $NH_4CuPO_4 \cdot H_2O$ can not be explained following the classification given by Eby and Hawthorne for copper oxysalts.[21] In this way, a new T—M=M—T cluster should be considered, where T is a tetrahedrally coordinated cation, M is a five coordinate cation, T—M represents corner sharing between five coordination polyhedra and tetrahedra and M=M represents edge sharing between five coordination polyhedra. So, we can conclude that the $NH_4CuPO_4 \cdot H_2O$ compound is the first infinite sheet copper oxysalt with the T—M=M—T layer topology.

Thermogravimetric study

The TGA and DTG curves of the title compound obtained under nitrogen atmosphere from room temperature to 600 °C are represented in Fig. 4. The thermal decomposition study shows two endothermic steps in the temperature range from 160 to 450 °C, which correspond to the mass loss of the ammonium and water molecules present in the structure (expt. 22.5%, calc. 23.0%).

The first endothermic step with an inclined section, between 160 °C and 225 °C, corresponds to a mass loss of approximately 10%. This fact can be attributed to the mass loss of the water molecule [eqn. (1)] with no appreciable loss of ammonia as was observed by Pysiak *et al.*[22]

$$NH_4CuPO_4 \cdot H_2O \rightarrow NH_4CuPO_4 + H_2O\uparrow \quad (1)$$

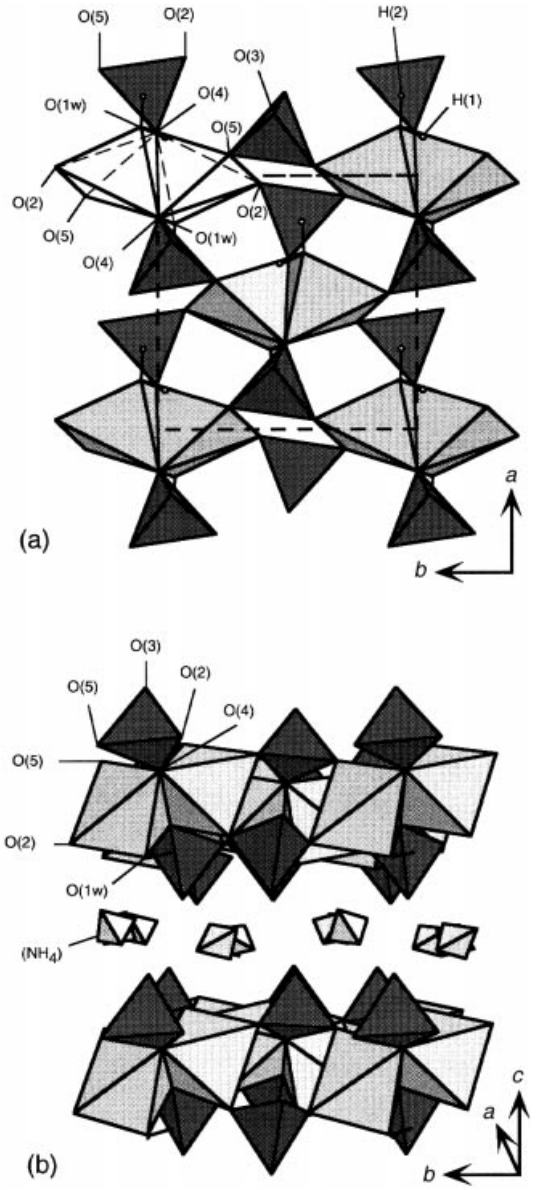

Fig. 1 Crystal structure of $NH_4CuPO_4{\cdot}H_2O$ (a) projected along [001] and (b) a perspective view along [100]

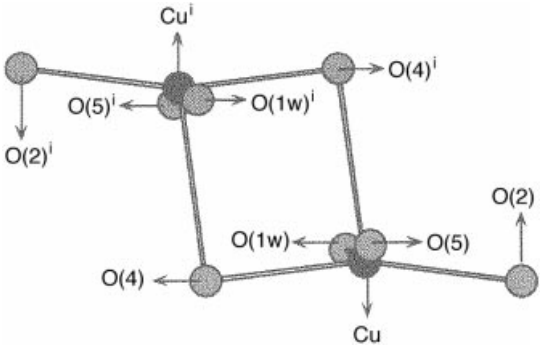

Fig. 2 View of the centrosymmetric $[Cu_2O_8]$ dimer present in the $NH_4CuPO_4{\cdot}H_2O$ compound

The second step, between 260 and 450 °C, corresponds to the deammoniation [eqn. (2)] and anion rearrangement [eqn. (3)] of the acid salt anion with evolution of the remaining water molecule and formation of diphosphate as the end product.

$$NH_4CuPO_4 \rightarrow CuHPO_4 + NH_3\uparrow \quad (2)$$

$$2CuHPO_4 \rightarrow Cu_2P_2O_7 + H_2O\uparrow \quad (3)$$

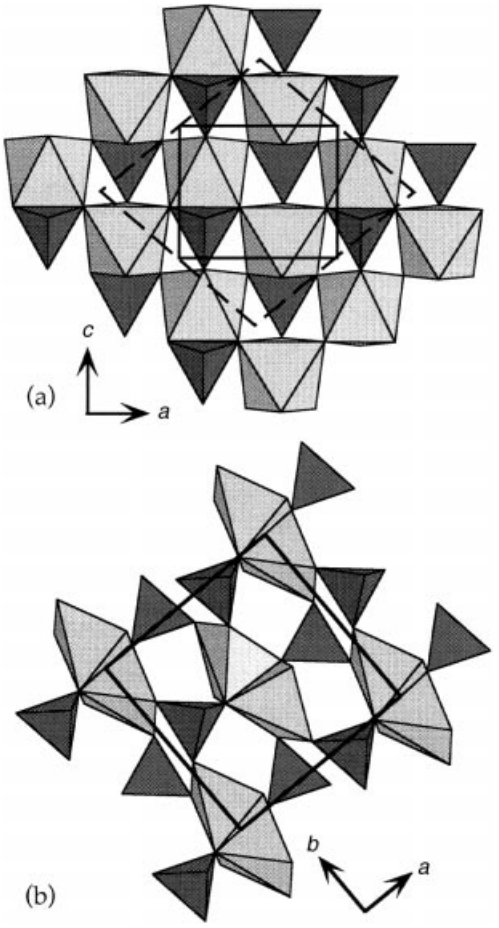

Fig. 3 Comparison between the layers present in (a) dittmarite and (b) $NH_4CuPO_4{\cdot}H_2O$. The solid lines represent the unit cells of the compounds. The dashed lines in (a) show the relation between the cells of both phases.

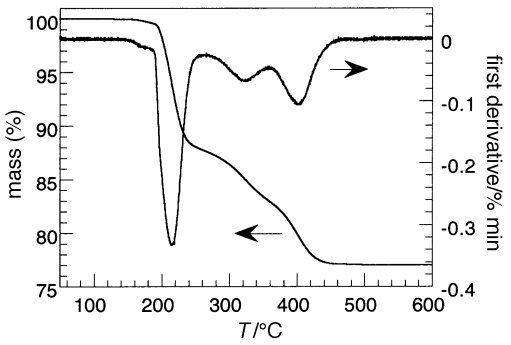

Fig. 4 TGA and DTG curves under nitrogen atmosphere of the $NH_4CuPO_4{\cdot}H_2O$ compound

The final product was identified by powder X-ray diffraction as $Cu_2P_2O_7$. The calculated cell parameters, $a = 6.876(2)$, $b = 8.115(1)$, $c = 9.162(1)$ Å and $\beta = 109.3(1)°$, are in excellent agreement with those previously reported by Effenberger [$a = 6.895(2)$, $b = 8.113(3)$, $c = 9.164(3)$ Å and $\beta = 109.6(1)°$].[23]

IR Spectroscopy

The IR spectrum of $NH_4CuPO_4{\cdot}H_2O$ presents a set of bands in the range 3000–3500 cm^{-1}, which can be assigned to the stretching vibration modes of the OH and NH groups, in good agreement with the presence of the ammonium group and the water molecule in the compound.

The band corresponding to the bending mode, $\delta(H-O-H)$, of the O—H group appears at 1615 cm^{-1}. Two bands at 1440 and 1470 cm^{-1} can also be observed which were ascribed to

the bending mode, $\delta(H-N-H)$, of the NH_4^+ group. For this compound the splitting observed is indicative of the existence of distortion in the NH_4^+ polyhedra.

Finally, the $\nu_{st}(PO_4)$ bands appear in the range 940–1100 cm^{-1}. These bands are split due to the distortion of the PO_4 tetrahedra in good agreement with the structural data. These results are confirmed by the presence of the PO_4 bending modes which are located in the 560–625 cm^{-1} range.

EPR Spectroscopy and magnetic properties

EPR spectra of the title compound were recorded on powdered samples at both X (4.2–300 K) and Q (100–300 K) bands and they are shown in Fig. 5 and 6. The X-band spectra are not well resolved due to a rather large linewidth and seem to correspond to an axial $\boldsymbol{g}$ tensor [Fig. 5(a)]. However, at the Q-band at room temperature (Fig. 6) the signal is clearly characteristic of a rhombic $\boldsymbol{g}$ tensor with the following main values: $g_1=2.339$, $g_2=2.157$ and $g_3=2.074$. These values are in good agreement with the topology of a distorted square pyramid exhibited by the $[CuO_5]$ chromophore, the lowest g value being higher than 2.04 as expected for an unpaired electron on a $d_{x^2-y^2}$ orbital.[24]

The X-band EPR spectra remain essentially unchanged, upon cooling the sample from 300 to 30 K [Fig. 5(a)]. At lower temperatures the linewidth rapidly increases and the spectrum becomes near isotropic at 4.2 K. The apparent g-value at this temperature is 2.185, close to the average value determined from the Q-band spectrum at room temperature.

The signal intensity increases when the temperature is lowered, reaches a maximum at about 6 K, and decreases at lower temperatures [see Fig. 5(b)]. Between 300 and 50 K the signal intensity shows a linear dependence upon $1/T$, as expected for a purely paramagnetic sample. Below 50 K, the observed behaviour is characteristic of an antiferromagnetic system. Moreover, the abrupt deviation from the Curie law suggests the presence of predominant short range interactions. This result is not *a priori* surprising, if one takes into account the presence of dimeric $[Cu_2O_8]$ entities in the title compound. However, two facts are important to note: (i) the signal becomes isotropic at low temperature, and (ii) the $\Delta M_s=2$ forbidden transition was not observed around 150 mT in spite of the presence of dimeric entities. These facts indicate that extensive exchange coupling could take place in the compound.

The thermal evolutions of both the magnetic molar susceptibility and $\chi_m T$ values are shown in Fig. 7. As the temperature is lowered the susceptibility increases until a maximum of 0.039 $cm^3\ mol^{-1}$, which is reached at 6 K, and then rapidly decreases (0.012 $cm^3\ mol^{-1}$ at 1.8 K). The high temperature data ($T>20$ K) are well described by a Curie–Weiss law ($\chi_m=C_m/T-\theta$), with $C_m=0.44\ cm^3\ K\ mol^{-1}$ and $\theta=-2.7$ K. The observed Curie constant agrees quite well with that calculated using the g value obtained from the EPR data (0.45 $cm^3\ K\ mol^{-1}$). The $\chi_m T$ product lies practically constant (0.44 $cm^3\ K\ mol^{-1}$) between 300 and 50 K, and decreases quickly when cooling to 1.8 K (0.022 $cm^3\ K\ mol^{-1}$). The negative θ value together with the continuous decrease of the effective magnetic moment observed when the temperature is lowered are indicative of the predominance of antiferromagnetic interactions in this compound.

Considering the structural features exhibited by this compound, three different exchange pathways could be *a priori* involved in the observed magnetic behaviour: (i) dimeric couplings *via* oxygen bridges, (ii) 2D interactions *via* phosphate groups which connect the dimeric $[Cu_2O_8]$ entities, and (iii) interlayer couplings *via* NH_4^+ cations. In fact, if we observe that the susceptibility tends to zero with temperature and that the decrease of the effective magnetic moment is extremely fast below 20 K, it could be considered that the observed magnetic behaviour appears to correspond to a system in which the short range (dimeric) interactions are predominant. In this way, and considering only dimeric couplings, one can easily estimate the exchange parameter J between Cu^{II} ions from the temperature at which the susceptibility reaches the maximum value [$T(\chi_{max})=5/4\ |J|/k$], as well as from the Weiss temperature ($\theta=J/2k$). The obtained J/k values are 4.8 and 5.3 K, respectively. The difference between the values is small enough to validate the hypothesis of a simple dimeric model although it suggests that other minor contributions may be involved.

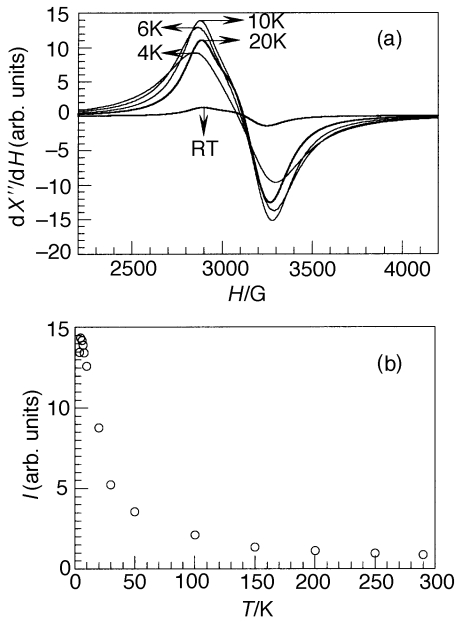

Fig. 5 (a) X-Band EPR spectrum of a powdered sample of $NH_4CuPO_4{\cdot}H_2O$ at different temperatures. (b) Thermal variation of the EPR signal intensity of $NH_4CuPO_4{\cdot}H_2O$.

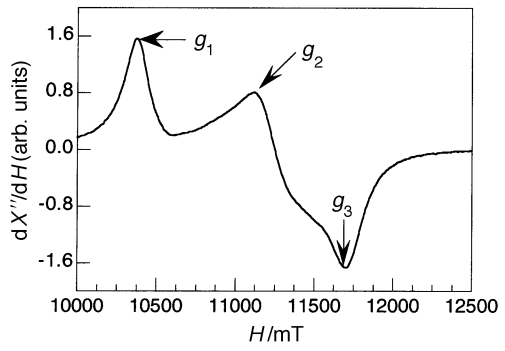

Fig. 6 Q-Band EPR spectrum of a powdered sample of $NH_4CuPO_4{\cdot}H_2O$ at room temperature

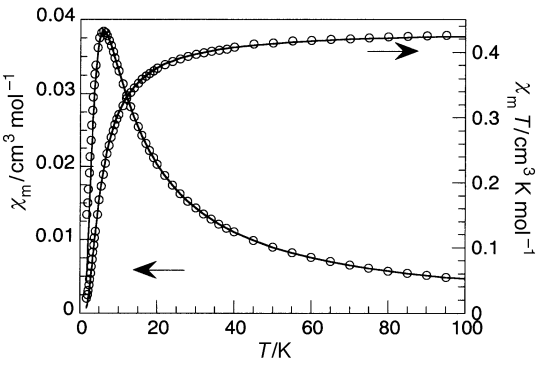

Fig. 7 Thermal variation of χ_m and $\chi_m T$ for $NH_4CuPO_4{\cdot}H_2O$: the circles are the experimental values and the full lines represent the theoretical values for dimeric systems (see text)

A more complete description of the observed magnetic behaviour may be obtained by using the Bleaney–Bowers equation for two copper atoms,[25] derived from the Heisenberg spin Hamiltonian ($H=-2J\boldsymbol{S}_1\boldsymbol{S}_2$) for two coupled $S=1/2$ ions:

$$\chi_m=\frac{Ng^2\beta^2}{kT}\left[\frac{1}{3+\exp(-2J/kT)}\right]$$

where the parameters have their usual meanings.

The best least-squares fit (solid lines in Fig. 7) is obtained with the parameter $J/k=-4.8$ K (3.3 cm^{-1}) and $g=2.16$. The agreement factor, defined as $SE=[\Phi/(n-K)]^{1/2}$ where n is the number of data points (73), K is the number of adjustable parameters (2), and Φ is the sum of squares of the residuals, is equal to 2.2×10^{-3}. The observed small J-value can be explained as a consequence of the arrangement of the Cu^{II} ions in this system. In Cu^{II} dimers it has been observed that when the bridging angles are close to 90° the interaction between the magnetic orbitals is small but not negligible, and therefore antiferromagnetic interactions could be expected.[26] So, in the title compound in which the bridging angle is 91.5° and the magnetic orbitals (mainly $d_{x^2-y^2}$) are in practically parallel planes (see Fig. 2) the orbital interactions transmitted through the O(4) atoms must be necessarily weak, giving rise to a small J value as was observed from the magnetic measurements.

The experimental and calculated results agree quite well, but the fit is not so good at lowest temperatures. Below 4 K the experimental susceptibility decreases more slowly than the calculated one. Besides, the calculated g-value is somewhat lower than that determined from the EPR spectra. Both facts can be attributed to the existence of weaker long range interactions. Attempts to evaluate the interdimeric interactions by mean of a J' parameter treated in the molecular field approximation lead to extremely low values without a significant improvement of the fit.

In the related $NH_4MPO_4{\cdot}H_2O$ (M = Co, Ni, Mn, Fe) compounds,[8–12,27] the observed magnetic behaviour corresponds mainly to that expected for 2D antiferromagnetic systems with significant interlayer interactions *via* ammonium groups. In those compounds, dimeric entities are not present as observed in the title one. Therefore, one can conclude that the magnetic behaviour of the $NH_4CuPO_4{\cdot}H_2O$ compound, in spite of its layered structure, is dominated by the interactions between the copper(II) ions forming the dimeric entities. A 2D ordering, as exhibited by the cited related compounds, may be reached at temperatures lower than 1.8 K.

Concluding remarks

A new layered copper phosphate, $NH_4CuPO_4{\cdot}H_2O$, has been obtained. This compound presents a layered structure, with copper phosphate sheets separated by NH_4^+ cations. The inorganic layers are formed by centrosymmetric dimers of CuO_5 edge-sharing square pyramids, crosslinked by the phosphate tetrahedra. This fact is different from that observed for the dittmarite family in which the $[MO_6]$ octahedra are separated by the phosphate groups. The five coordination to the copper(II) ion causes a distortion in comparison to the dittmarite structure. As a result, the intralayer unit cell parameters of the $NH_4CuPO_4{\cdot}H_2O$ compound are almost equivalent to the intralayer unit cell diagonals of dittmarite. The interlayer distances are similar for both compounds, however an interlayer displacement is observed. This fact gives rise to a change in the crystalline system from rhombic to monoclinic. As far as we are aware, the title compound is the first infinite sheet copper oxysalt with T—M=M—T layer topology. The spectroscopic data for the layered compound confirm the high symmetry of the PO_4 and NH_4 groups. EPR data and magnetic studies show antiferromagnetic interactions and the presence of predominant short range interactions in this compound. The antiferromagnetic behaviour can be explained by a dimeric system. A 2D ordering, as exhibited by other related compounds, may be reached at temperatures lower than 1.8 K.

A. P. thanks the Basque Government/Eusko Jaurlaritza for a Doctoral Fellowship. This work was financially supported by the Basque Country Grant PI-9439, which we gratefully acknowledge.

References

1 T. Kanazawa, *Inorganic Phosphate Materials*, Elsevier, Tokyo, 1993.
2 V. Vance Guliants, J. B. Benziger and S. Sundaresan, *Chem. Mater.*, 1994, **6**, 353.
3 D. Papoutsakis, J. E. Jackson and D. G. Nocera, *Inorg. Chem.*, 1996, **35**, 800.
4 Y. Ding, D. J. Jones, P. M. Torres and J. Roziere, *Chem. Mater.*, 1995, **7**, 562.
5 C. V. Kumar, A. Chaudhari and G. L. Rosenthal, *J. Am. Chem. Soc.*, 1994, **116**, 403.
6 B. Shpeizer, D. M. Poojary, K. Ahn, C. E. Runyan and A. Clearfield, *Science*, 1994, **266**, 1357.
7 D. Tranqui, A. Durif, J. C. Guitel and M. T. Averbuch-Pouchot, *Bull. Soc. Fr. Mineral. Crystallogr.*, 1968, **91**, 10.
8 S. G. Carling, P. Day and D. Visser, *Inorg. Chem.*, 1995, **34**, 3917.
9 A. Goñi, J. L. Pizarro, L. M. Lezama, G. E. Barberis, M. I. Arriortua and T. Rojo, *J. Mater. Chem.*, 1996, **6**, 421.
10 S. G. Carling, P. Day and D. Visser, *Solid State Commun.*, 1993, **88**, 132.
11 J. E. Greendan, K. Reubenbauer, T. Birchall, M. Ehlert, D. R. Corbin and M. A. Subramanian, *J. Solid State Chem.*, 1988, **77**, 376.
12 S. G. Carling, P. Day and D. Visser, *Acta Crystallogr., Sect. A*, 1990, **46**, 278.
13 H. Basset and W. Bedwell, *J. Chem. Soc.*, 1933, 854.
14 Xtal 3.2 Reference Manual, ed. S. R. Hall, H. D. Flack and J. M. Stewart, Universities of Western Australia, Australia, Geneva, Switzerland and Maryland, USA, 1992.
15 D. T. Cromerand and J. T. Waber, *International Tables For X-ray Crystallography*, Vol. 4, Kynoch Press, Birmingham, 1974.
16 G. M. Sheldrick, SHELX 86, *Acta Crystallogr., Sect. A*, 1990, **46**, 467.
17 G. M. Sheldrick, SHELXL-93, Program for the Refinement of Crystal Structures, University of Göttingen, Germany, 1993.
18 M. Nardelli, PARST, *Comput. Chem.*, 1983, **7**, 95.
19 J. M. Stewart, F. A. Kundel and J. C. Baldwin, The X-ray System, Computer Science Center, Univ. of Maryland, College Park, MA, USA, 1976.
20 E. Dowty, ATOMS: A Computer Program for Displaying Atomic Structures. Shape Software, 521 Hidden Valley Road, Kingsport, TN, 1993.
21 R. K. Eby and F. C. Hawthorne, *Acta Crystallogr., Sect. B*, 1993, **49**, 28.
22 J. Pysiak, E. E. Prodan, V. V. Samuskevich, B. Pacewska and N. A. Shkorik, *Thermochim. Acta*, 1993, **222**, 91.
23 H. Effenberger, *Acta Crystallogr., Sect. C*, 1990, **46**, 691.
24 B. J. Hathaway and D. E. Billing, *Coord. Chem. Rev.*, 1970, **5**, 143.
25 B. Bleaney and K. D. Bowers, *Proc. R. Soc. London, Ser. A,* 1952, **214**, 451.
26 P. Alemany and S. Alvarez, *Chem. Mater.*, 1990, **2**, 723.
27 G. Villeneuve, J. L. Pizarro, J. M. Dance, M. I. Arriortua, T. Rojo and R. Kuentzler, *J. Magn. Magn. Mater.*, 1990, **83**, 478.

Paper 7/08238J; *Received* 17*th November*, 1997